International Journal of Engineering

Journal Homepage: www.ije.ir

Corrosion Behavior Evaluation of Nanolayered CrN/CrAlN Coatings on Titanium and Ti6Al4V Substrates

N. Fereshteh-Saniee[a], H. Elmkhah[*a], M. Molaei[a], A. Zolriasatein[b]

[a] Department of Materials Engineering, Bu-Ali Sina University, Hamedan, Iran
[b] Non-metallic Materials Research Group, Niroo Research Institute (NRI), Tehran, Iran

ABSTRACT

In recent years, implants are used as prostheses to replace and protect bone. Titanium, as an implantable material, needs to improve corrosion and wear properties for better performance. Therefore, in the current study nitride coatings were applied with the aim of improving corrosion and wear properties. Cathodic arc evaporation physical vapor deposition (CAE-PVD) technique was used to deposit nanolayered CrN/CrAlN coatings on commercially pure titanium and Ti6Al4V substrates for biomaterial applications. X-ray diffraction (XRD) was used to characterize the crystal structure of the coating, and scanning electron microscopy (SEM) and field emission scanning electron microscopy (FESEM) were utilized to observe the surface morphology and cross-section of the coating. The coating adhesion was measured according to VDI 3198 standard using a Rockwell-C indenter. The corrosion behavior was evaluated by potentiodynamic polarization and spectroscope electrochemical impedance in Ringer's solution. The results showed that the nanolayered coating changed the corrosion potential from -0.368 V to -0.054 V for the titanium sample and from -0.405 V to -0.028 V for the Ti6Al4V specimen. Additionally, the corrosion current density was reduced to about ***one-eighth*** and a third for the titanium and Ti6Al4V coated samples, respectively. The capacitor circle diameters increased due to the deposition of CrN/CrAlN coating, demonstrating enhanced corrosion behavior of the coated samples compared to uncoated specimens, as the coating acted as a barrier against corrosive liquids accessing the substrate.

doi: 10.5829/ije.2024.37.01a.12

1. INTRODUCTION

As an implant material, titanium has been widely used in various medical applications due to its excellent biocompatibility properties, including the spontaneous formation of a stable and dense oxide layer on its surface. Additionally, titanium and its alloys have favorable mechanical, physical, and biological properties for implantation (1, 2). The desired characteristics of titanium and its alloys include a relatively suitable elastic modulus, good formability and machineability, excellent biocompatibility, and superior corrosion resistance compared to stainless steel and cobalt base-alloys (3). Therefore, damaged tissues can be replaced by titanium and its alloys in various situations (1).

However, pure titanium and Ti6Al4V alloy have some drawbacks such as low wear resistance, the possibility of passive layer interaction with H_2O (4), weak shear strength, and difficult production technique. Moreover, the surface oxide layer creates high friction and intensified wear rate for these materials. When the protective coating breaks down, the titanium substrate gets exposed to the surrounding environment, and if the protective layer is not repaired, the titanium is strongly exposed to shear stresses which can result in the formation of cold sores between it and the surrounding joints. Alternative separation and reformation of the oxide layer on the titanium surface consume the implant material. By continuing this phenomenon, the surface roughness increases, hard and coarse particles are created, causing abrasive wear at the implant surface (5). The worn particles can cause blood clots and swelling of the surrounding regions, leading to implant replacement and serious patient suffering (6, 7). Additionally, the

Corresponding Author Email: h.elmkhah@basu.ac.ir (H. Elmkhah)

higher elastic modulus of this material compared to that of bone can cause the stress shielding phenomenon (8). Moreover, using Ti6Al4V alloy as a long-term implant can create problems due to potential releases of vanadium and aluminum ions which may cause cellular toxicity and tissue noxious reactions (6, 7). Therefore, improving the corrosion resistance of titanium implants is essential to increase their biocompatibility and prolong their life (9, 10).

Surface modification is a method to enhance the chemical, mechanical, and biomedical properties of titanium composition. It can be achieved by chemical or mechanical methods (11, 12), such as shot penning (13, 14), sol gel (15), chemical vapor deposition (16), plasma-assisted chemical vapor deposition (17), thermal sputtering (18), electrochemical plating (19, 20), and physical vapor deposition (21-23). Among the above-mentioned techniques, cathodic arc evaporation, due to the creation of uniform properties such as continuous, dense, and homogeneous coating, high adhesion to the substrate, material structure protection, and the possibility of multilayer coating deposition, can be used to form nitride coatings. Nitride coatings have several desirable properties, including high chemical stability, favorite hardness and adhesion, excellent resistance to corrosion and wear, as well as good hammering (24).

Studies have shown that nitride coatings deposited on titanium and its alloys using cathodic arc evaporation can improve their corrosion resistance. Olia et al. (25) deposited CrN/CrAlN and TiN/TiAlN coatings on stainless steel using the cathodic arc evaporation method, and corrosion tests in 3.5% NaCl solution showed that Ecoor of coated samples shifted to more positive potential. Khan et al. (26) also coated stainless steel using TiN, CrN, AlTiN, and AlCrN and evaluated their electrochemical behaviors. The coated samples had better corrosion resistance, with the CrN coating showing the best corrosion resistance. Additionally, different nitride coatings were deposited on steel substrates using cathodic arc evaporation, and the corrosion behavior was evaluated in 0.1M Na_2SO_4 and 0.1M NaCl environments (27). The Ti-based coatings exhibited best corrosion resistance and surface properties.

Several studies have been performed within the field of CrAlN coatings research (16, 28). The distinctive aspect of this study, in comparison to previous research, involves the utilization of two distinct substrates, including pure Ti and Ti6Al4V, and the subsequent evaluation of their respective corrosion characteristics in relation to one another. To enhance the performance of titanium as an implantable material, it is imperative to address the concerns regarding its corrosion and wear properties. Hence, in the present investigation, nitride coatings were employed with the objective of enhancing the corrosion resistance and wear characteristics. Therefore, the aim of this investigation is to study and

assess the corrosion behavior of CrN/CrAlN coating deposited using cathodic arc evaporation on titanium and Ti6Al4V substrates in the Ringer solution.

2. MATERIALS AND METHODS

2. 1. Surface Preparation and Coating Parameters
To achieve a high-quality and desired surface for coating, pure commercial titanium and Ti6Al4V alloy samples were prepared in sheet form and polished using 120 to 3000 grit sandpapers. Following this, the samples were washed in an acetone solution using an ultrasound device for ten minutes. Finally, CrN/CrAlN nano-coatings were deposited on the titanium and Ti6Al4V substrate using the cathodic arc evaporation method. The coating parameters are briefly summarized in Table 1.

2. 2. Coating Characterization
The X-ray diffraction device (1730 PW Philips and PANalytical) was used to identify the structures and types of coating phases formed. The angle diffraction was selected in the range of 10-80 degrees with a step size of 0.05 degrees. To observe the cross-section of the coating, the titanium sample was first cut with a guillotine and then prepared for photography after the mount treatment, sanding, and polishing. A gold coating was applied to make the mount conductive. The surface morphology and cross-section of the coating were observed using scanning electron microscopy (840A-JSM, Jeol) and field emission scanning electron microscopy (Czech, TESCAN, MIRA3, FESEM), and the energy distribution spectrum was obtained by SAMX, France. The surface roughness was measured using a roughness meter (Roughness Tester PCE RT 2200). The adhesion test was carried out by applying 150 N force for 25 seconds using a Rockwell-C indenter and VDI3198 standard. The impression created by the indenter was observed via optical microscopy. According to the VDI3198 standard, coatings having adhesion conditions HF1 to HF3 are acceptable, whereas HF4 to HF6 states could be rejected. The classification of coating adhesion based on the VDI3198 standard is illustrated in Figure 1.

TABLE 1. The coating process parameters used in the present work

Working pressure (torr)	5×10^{-3}
Target electrical current (A)	100
Substrate-target distance (cm)	15
Deposition time (min)	90
Rotational speed of specimens (rpm)	5
Substrate bias voltage (V)	-100
Duty cycle (%)	50
Deposition temperature (ºC)	200
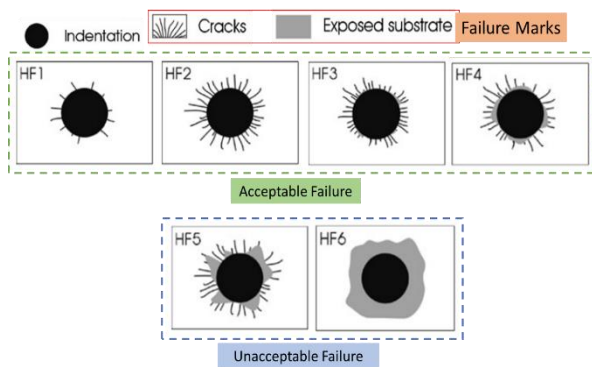
Figure 1. The classification of coating adhesion according to the VDI3198 standard

Figure 2. XRD pattern of CrN/CrAlN coating

2. 3. Corrosion Test   The electrochemical impedance spectroscopy (EIS) and potentiodynamic polarization (PDP) tests using a potentiostat instrument (μAutolab, III/FRA2, made in the Netherlands) were conducted to evaluate the corrosion behavior of uncoated and CrN/CrAlN coated pure Ti and Ti6Al4V alloy substrates in a physiologic Ringer's solution (pH 7.4). The samples were set up according to the conventional three-electrode cell configuration. The EIS tests were operated with a signal amplitude of 10 mV and a frequency ranging from 100000 to 0.01 Hz when the open circuit potential (OCP) was stable, which occurred after 2 hours. The EIS test data were analyzed using NOVA software (version 2.1.3). The PDP test was performed at a scan rate of 1 mV/s, starting from −250 mV below the OCP. The PDP curves were analyzed using the Tafel extrapolation technique. The SEM was applied to study the corrosion surface morphologies characteristics of specimens.

3. RESULTS AND DISCUSSIONS

3. 1. Microstructure of the Coating   Figure 2 displays the X-ray diffraction patterns of the Ti substrate and Ti coated with CrN/CrAlN. The latter pattern includes CrN and AlN with a face center cubic (FCC) structure, as well as the Cr_2N and substrate with a hexagonal structure. For CrN and AlN phases of this coating, diffraction peaks associated with (111), (200), and (220) planes occur at 37.6, 43.7, and 63.5 angles. On the other hand, diffraction peaks of the titanium are at 35, 38.4, and 40.1 angles in relation to (100), (002), and (101) planes. According to the observed pattern, the coating's referred orientation is (200), consistent with previous researchers' reports (29, 30).

3. 2. Suface Morphology and Coating Thickness
Figure 3 ehibits the SEM images of the CrN/CrAlN coating urface. Macroparticles can be observed on the
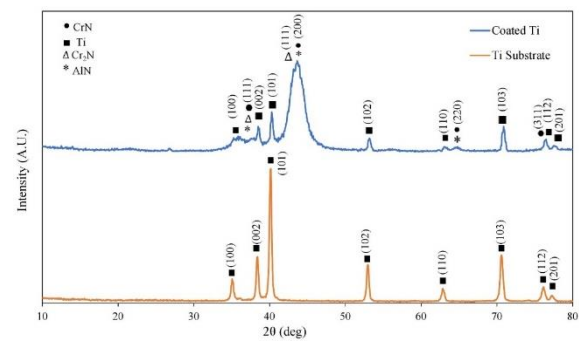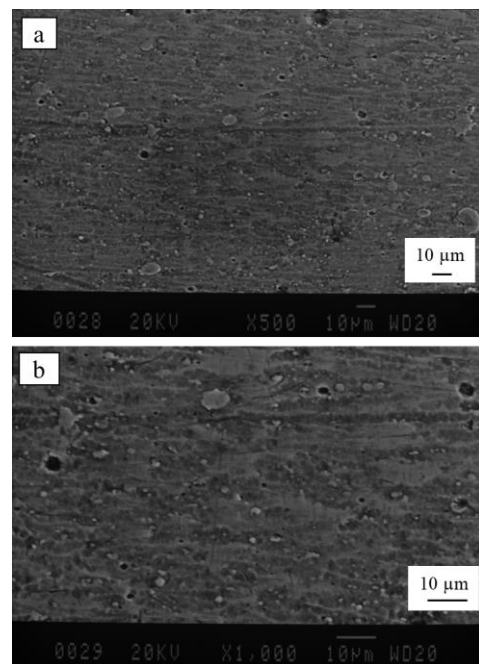
Figure 3. SEM images of CrN/CrAlN surface coating with different magnifications a) ×500, b) ×1000

surface. The presence of macroparticles is normal in the cathodic arc evaporation process and causes a partial increase in the roughness of the coated samples compared with the uncoated samples. The factors affecting the number and size of microparticles include the rate of evaporation of the target material, the deposition rate, and accumulation of the coating on the metal substrate (31). Figure 4 illustrates the FESEM images of the cross-section of the coating. The images display a continuous and dense coating microstructure. Additionally, the lack of a separation line between the substrate and coating reveals a high adhesion of the coating to the substrate. Moreover, the CrN and CrAlN nanolayers were compactly adhered together, without any visible cracks or holes in their interface resulting in improved corrosion resistance. The created coating possesses a nanostructure with a fully homogeneous, 2-micron thickness, and

compact layers of CrN and CrAlN. Figure 5 shows the energy distribution spectroscopy (EDS) of the coated samples. The analysis was performed from the surface to the depth of the sample and includes Cr, Al, N, and Ti elements.

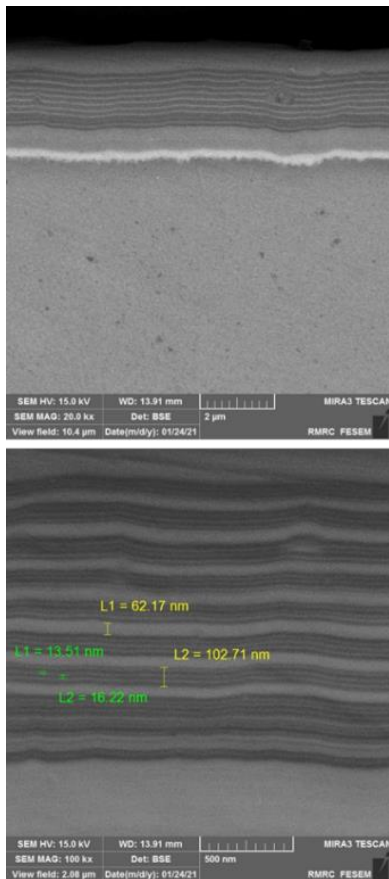### 3. 3. Surface Roughness and Adhesion
The coating adhesion was evaluated via Rockwell-C test in the present investigation. The condition of the coating surrounding the impression of the indenter was observed using an optical microscope. Figure 6 displays the images obtained from the adhesion tests for titanium and Ti6Al4V samples coated with CrN/CrAlN. No cracks or disintegration exist around the impression of the indenter, indicating a high level of coating adhesion in the HF1 group. Table 2 summarizes the surface roughness data for coated and uncoated samples. The coated samples have a higher roughness than the uncoated samples due to the nature of the cathodic arc evaporation process, explained in section 2.3.
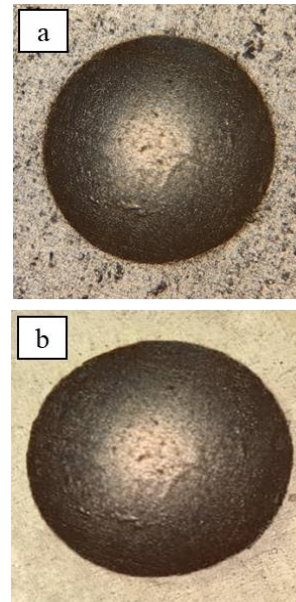
3. 4. Electrochemical Behavior
The corrosion behavior of the titanium and Ti6Al4V substrates before and after being coated with nanolayer CrN/CrAlN
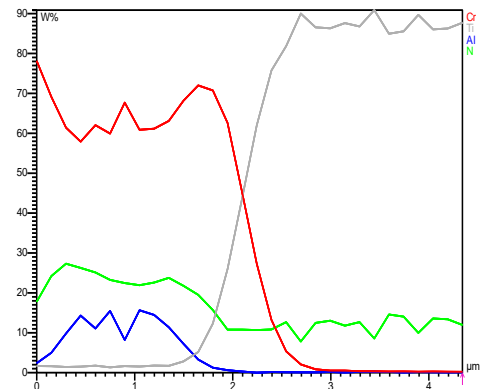
Figure 5. EDS line analysis of titanium sample with CrN/CrAlN coating


Figure 6. Optical microscope images of the indenter impression on coating ×100 magnification, (a) commercial pure titanium, and (b) Ti6Al4V

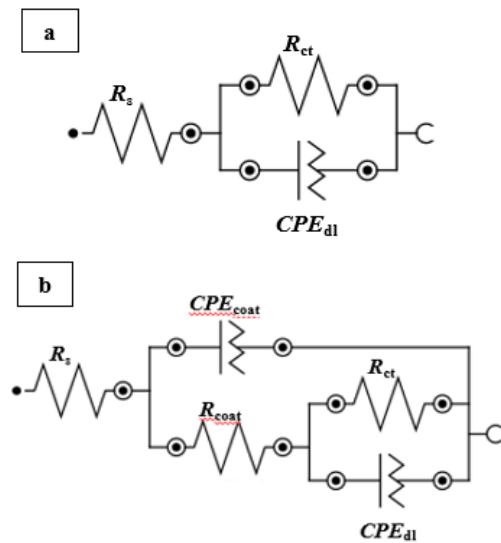**TABLE 2.** Surface roughness values of uncoated and CrN/CrAlN coated titanium and Ti6Al4V samples

Sample	R_a (µm)	R_z (µm)	R_{max} (mm)
Titanium	0.169	0.893	0.02
CrN/CrAlN coated titanium	0.221	1.220	0.04
Ti6Al4V	0.125	1.186	0.03
CrN/CrAlN coated Ti6Al4V	0.158	1.374	0.04

coatings was evaluated by EIS and PDP tests in the physiological Ringer's solution. Figure 7 illustrates the EIS test results in the form of Nyquist and Bode plots for uncoated and CrN/CrAlN coated titanium and Ti6Al4V substrates samples.

Figure 4. FESEM images of the cross section of CrN/CrAlN coating with different magnifications
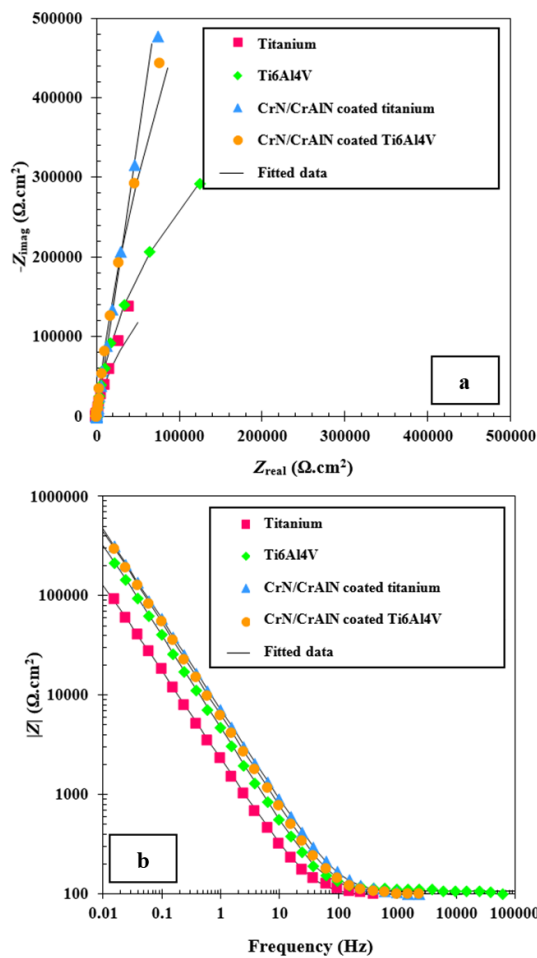
Figure 7. (a) Nyquist and (b) Bode plots of uncoated and CrN/CrAlN coated pure Ti and Ti6Al4V alloy substrates after 2 hours of exposure to physiological Ringer's solution

Figure 8. Equivalent circuits used to fit the EIS data of (a) uncoated and (b) CrN/CrAlN coated pure Ti and Ti6Al4V alloy substrates

The Nyquist plots of all uncoated and coated substrates (Figure 7 (a)) showed an uncompleted semicircle-like shape, while those for CrN/CrAlN coatings were larger in diameter. As can be observed in Bode plots of specimens (Figure 7 (b)), the uncoated titanium and Ti6Al4V indicated only one time constant, which is related to the capacitive behavior of the electrical double layer (Cdl) and the charge transfer resistance (Rct) of the surface oxide layer. However, there were two-time constants in Bode plots of the CrN/CrAlN coated samples, representing the capacitive behavior of the coatings and the electrical double layers. Moreover, at high-frequency regions, the frequency independency of the absolute impedance values suggested pure resistance behavior of specimens. The experimental impedance data of the uncoated and CrN/CrAlN coated titanium and Ti6Al4V substrates were fitted utilizing the equivalent circuit models displayed in Figure 8 (a) and (b), respectively. In these models, Rs, Rct, and Rcoat are respectively ascribed to
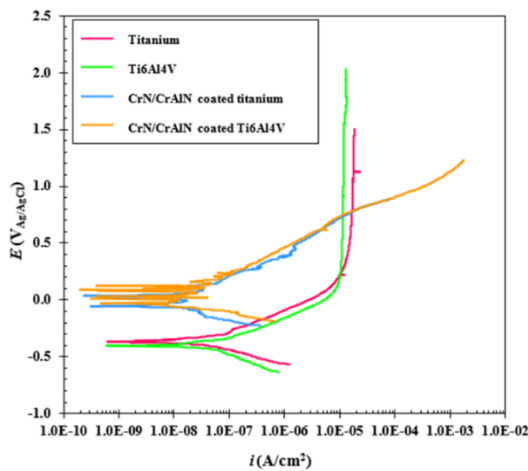
Ringer's solution resistance, charge transfer resistance (at the interface of substrate/Ringer's solution), and coating resistance (at the interface of coating/Ringer's solution). Moreover, CPEdl and CPEcoat are assigned to the constant phase elements of the electrical double layer and the coating capacitance, respectively. Generally, the CPE is employed in the circuit to compensate for the deviation of Cdl and Ccoat from ideal capacitive behavior due to the surface inhomogeneity (32, 33). The equivalent circuits fitted parameters are reported in Table 3. According to Table 3, it was found that the Rct values of CrN/CrAlN coated titanium and Ti6Al4V substrates (2.27 and 2.09 MΩ.cm^2, respectively) were higher than that of the uncoated samples (0.20 and 0.66 MΩ.cm^2 for titanium and Ti6Al4V substrates, respectively) which indicated improved anticorrosion properties of titanium and Ti6Al4V after being modified with nanolayer CrN/CrAlN coatings. Furthermore, when comparing CrN/CrAlN coated titanium and Ti6Al4V specimens with each other, the former presented higher Rct and lower Rcoat values. The PDP curves of uncoated and CrN/CrAlN coated titanium and Ti6Al4V substrates are indicated in Figure 9. For both titanium and Ti6Al4V substrates specimens, because of the formation of a surface passive oxide layer, the passive behavior was observed. The Ecorr, corrosion current density (icorr), anodic and cathodic slopes (βa and βc, respectively), and polarisation resistance (Rp) values of specimens derived from the PDP curves utilizing the Tafel extrapolation technique are summarized in Table 4. The Rp values of specimens were calculated using the Stern-Geary equation (34). While the Ecorr reflects the tendency of

TABLE 3. Simulated EIS parameters for uncoated and CrN/CrAIN coated titanium and Ti6AI4V substartes in physicological Ringer's solution

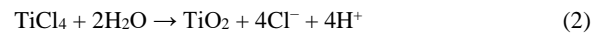| Sample	R_s ($\Omega.cm^2$)	CPE_{dl} ($\mu F/cm^2$)	n_{dl}	R_{ct} ($M\Omega.cm^2$)	CPE_{coat} ($M\Omega.cm^2$)	n_{coat}	R_{coat} ($K\Omega.cm^2$)
Titanium	100.08	85.42	0.88	0.20	-	-	-
CrN/CrAIN coated titanium	102.98	26.13	0.91	2.27	127.18	0.87	1.30
Ti6AI4V	111.78	38.34	0.93	0.66	-	-	-
CrN/CrAIN coated Ti6AI4V	102.87	28.44	0.92	2.09	105.02	0.81	2.03

TABLE 4. The E_{corr} and i_{corr} values of uncoated and CrN/CrAIN coated titanium and Ti6AI4V substartes

Sample	E_{corr} (mV)	i_{corr} ($\mu A/cm^2$)	β_a	β_c	R_p ($K\Omega.cm^2$)
Titanium	100.08	85.42	0.88	0.20	-
CrN/CrAIN coated titanium	102.98	26.13	0.91	2.27	127.18
Ti6AI4V	111.78	38.34	0.93	0.66	-
CrN/CrAIN coated Ti6AI4V	102.87	28.44	0.92	2.09	105.02

Figure 9. The classification of coating adhesion according to the VDI3198 standard

dissolution and stability, the icorr represents the corrosion rate. So, the lower the icorr and the more positive the Ecorr, the higher the corrosion resistance (29, 31, 35). The Ecorr and icorr values of CrN/CrAlN coated samples were respectively nobler and lower than those of uncoated ones, showing a remarkable enhancement in corrosion resistance of titanium and Ti6Al4V substrates after being coated with nanolayer CrN/CrAlN coatings. Titanium is corroded under the formation of soluble titanium oxychloride complexes and the consumption of the passive oxide layer by Cl− corrosive ions (36). According to Liang et al. (37), the following anodic and cathodic reactions happen during the corrosion of titanium and Ti6Al4V in Ringer's solution:
Anodic reactions:

$$Ti + 4Cl^- \rightarrow TiCl_4 + 4e^- \tag{1}$$

$$TiCl_4 + 2H_2O \rightarrow TiO_2 + 4Cl^- + 4H^+ \tag{2}$$

Cathodic reaction:

$$O_2 + 2H_2O + 4e^- \rightarrow 4OH^- \tag{3}$$

The CrN/CrAlN coating can act as a barrier against corrosion, not allowing direct contact of the corrosive solution with the titanium substrate. The improved structural density due to the increased number of interfaces in multilayer coatings can significantly enhance the corrosion resistance of the substrate compared with single-layer ones (29, 38). Although the Ti6Al4V substrate possessed a more negative Ecorr value (−405 mV) than that of titanium (−368 mV), the icorr value of Ti6Al4V (0.0278 µA/cm^2) was lower than the icorr value of titanium (0.0399 µA/cm^2), suggesting better anticorrosion behavior of Ti6Al4V. The α + β two-phase structure of Ti6Al4V with additional Al and V promotes its anodic passivation and increases its corrosion resistance compared with titanium (37). However, after being coated with CrN/CrAlN coatings, titanium exhibited more negative Ecorr (−54 mV) and lower icorr (0.0046 µA/cm^2) values than Ti6Al4V (with Ecorr and icorr values of −28 mV and 0.0086 µA/cm^2, respectively). Therefore, the corrosion resistance (Rp) of specimens was increased in the following order: uncoated titanium (64.842 KΩ.cm^2) < uncoated Ti6Al4V (93.064 KΩ.cm^2) < CrN/CrAlN coated Ti6Al4V (362.137 KΩ.cm^2) < CrN/CrAlN coated titanium (581.472 KΩ.cm^2).

Figure 10 shows the SEM surface morphologies of CrN/CrAlN coated titanium and Ti6Al4V substrates specimens after the corrosion test. Although some small
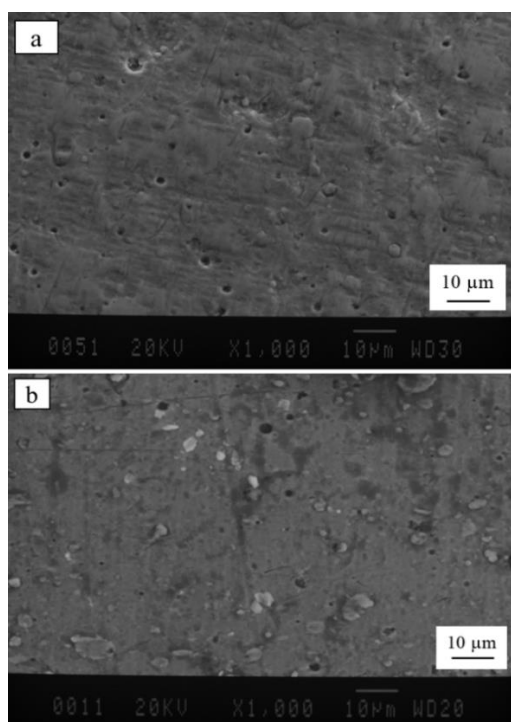
Figure 10. SEM surface morphologies of CrN/CrAlN coated specimens of (a) pure Ti and (b) Ti6Al4V alloy substrates after the corrosion test

corrosion pits were formed and no crack was seen on both coated surfaces, it seems that the CrN/CrAlN coated titanium underwent less damage compared to the coated Ti6Al4V. This showed the lower corrosion susceptibility of coated titanium in physiological Ringer's solution, as earlier discussed. Pits are formed because the coatings defects including cavities and macroparticles provide a direct path for corrosive ions to contact with the substrate (31-33). It can be concluded that pitting was the main corrosion mechanism of the specimens.

4. CONCLUSION

In this study, arc evaporation method was used to deposit CrN/CrAlN nanolayer coating on titanium and Ti6Al4V substrates. The results from the corrosion behavior evaluation of the coated and uncoated samples in Ringer's solution demonstrated that the deposited coating changed the corrosion potential from -0.386 V to -0.054 V for titanium and from -0.405 V to -0.0287 V for Ti6Al4V. In addition, the current density was reduced to about one-eighth and third for coated titanium and Ti6Al4V samples, respectively. Moreover, the increased capacitator circle diameters due to the deposition of CrN/CrAlN coating indicated improved corrosion behavior of the coated samples compared to the uncoated specimens.

5. REFERENCES

1. Renganathan G, Tanneru N, Madurai SL. Orthopedical and biomedical applications of titanium and zirconium metals. Fundamental biomaterials: metals: Elsevier; 2018. p. 211-41.

2. Kuphasuk C, Oshida Y, Andres CJ, Hovijitra ST, Barco MT, Brown DT. Electrochemical corrosion of titanium and titanium-based alloys. The Journal of prosthetic dentistry. 2001;85(2):195-202. 10.1067/mpr.2001.113029

3. Munsch M. Laser additive manufacturing of customized prosthetics and implants for biomedical applications. Laser additive manufacturing: Elsevier; 2017. p. 399-420.

4. Nematov D, Kholmurodov K, Husenzoda M, Lyubchyk A, Burhonzoda A. Molecular Adsorption of H2O on TiO2 and TiO2: Y Surfaces. Journal of Human, Earth, and Future. 2022;3(2):213-22.

5. Ramakrishna S, Ramalingam M, Kumar TS, Soboyejo WO. Biomaterials: a nano approach: CRC press; 2016.

6. Gomes CC, Moreira LM, Santos VJ, Ramos AS, Lyon JP, Soares CP, et al. Assessment of the genetic risks of a metallic alloy used in medical implants. Genetics and molecular biology. 2011;34:116-21. 10.1590/S1415-47572010005000118

7. Moghadasi K, Isa MSM, Ariffin MA, Raja S, Wu B, Yamani M, et al. A review on biomedical implant materials and the effect of friction stir based techniques on their mechanical and tribological properties. Journal of Materials Research and Technology. 2022;17:1054-121. 10.1016/J.JMRT.2022.01.050

8. Zhang L-C, Chen L-Y, Wang L. Surface modification of titanium and titanium alloys: technologies, developments, and future interests. Advanced Engineering Materials. 2020;22(5):1901258. 10.1002/adem.201901258

9. Prando D, Brenna A, Diamanti MV, Beretta S, Bolzoni F, Ormellese M, et al. Corrosion of titanium: Part 1: Aggressive environments and main forms of degradation. Journal of applied biomaterials & functional materials. 2017;15(4):e291-e302. 10.5301/jabfm.5000387

10. Mohammed MT, Khan ZA, Siddiquee AN. Surface modifications of titanium materials for developing corrosion behavior in human body environment: a review. Procedia Materials Science. 2014;6:1610-8. 10.1016/j.mspro.2014.07.144

11. Mozetič M. Surface modification to improve properties of materials. Mdpi; 2019. p. 441.

12. Xue T, Attarilar S, Liu S, Liu J, Song X, Li L, et al. Surface modification techniques of titanium and its alloys to functionally optimize their biomedical properties: thematic review. Frontiers in Bioengineering and Biotechnology. 2020;8:603072. 10.3389/fbioe.2020.603072

13. Li N-b, Sun S-j, Bai H-y, Xu W-h, Xiao G-y, Zhang Y-l, et al. Evolution of nano/submicro-scale oxide structures on Ti6Al4V achieved by an ultrasonic shot peening-induction heating approach for high-performance surface design of bone implants. Journal of Alloys and Compounds. 2020;831:154876. 10.1016/j.jallcom.2020.154876

14. Yang Q, Zhou W, Zheng X, Niu Z, Li Z, Zou B, et al. Investigation of shot peening combined with plasma-sprayed CuNiIn coating on the fretting fatigue behavior of Ti-6Al-4V dovetail joint specimens. Surface and Coatings Technology. 2019;358:833-42. 10.1016/j.surfcoat.2018.12.006

15. Jaafar A, Hecker C, Árki P, Joseph Y. Sol-gel derived hydroxyapatite coatings for titanium implants: A review. Bioengineering. 2020;7(4):127. 10.3390/bioengineering7040127

16. Din S, Shah M, Sheikh N. Tribological performance of titanium alloy Ti–6Al–4V via CVD–diamond coatings. Journal of Superhard Materials. 2018;40:26-39. 10.1016/j.ceramint.2022.09.286

17. Cho Y-S, Liao L-K, Hsu C-H, Hsu Y-H, Wu W-Y, Liao S-C, et al. Effect of substrate bias on biocompatibility of amorphous carbon coatings deposited on Ti6Al4V by PECVD. Surface and Coatings Technology. 2019;357:212-7. 10.1016/j.surfcoat.2019.07.011

18. Gan JA, Berndt CC. Thermal spray forming of titanium and its alloys. Titanium Powder Metallurgy. 2015:425-46. 10.1016/B978-0-12-800054-0.00023-X

19. Rao CR, Pushpavanam M. Electroless deposition of platinum on titanium substrates. Materials Chemistry and Physics. 2001;68(1-3):62-5. 10.1016/S0254-0584(00)00268-6

20. Mahmoud S. Electroless deposition of nickel and copper on titanium substrates: Characterization and application. Journal of alloys and Compounds. 2009;472(1-2):595-601. 10.1016/j.jallcom.2008.05.079

21. Bahi R, Nouveau C, Beliardouh NE, Ramoul CE, Meddah S, Ghelloudj O. Surface performances of Ti-6Al-4V substrates coated PVD multilayered films in biological environments. Surface and Coatings Technology. 2020;385:125412. 10.1016/j.surfcoat.2020.125412

22. Uddin GM, Jawad M, Ghufran M, Saleem MW, Raza MA, Rehman ZU, et al. Experimental investigation of tribo-mechanical and chemical properties of TiN PVD coating on titanium substrate for biomedical implants manufacturing. The International Journal of Advanced Manufacturing Technology. 2019;102:1391-404. 10.1007/s00170-018-03244-2

23. Ewald A, Glückermann SK, Thull R, Gbureck U. Antimicrobial titanium/silver PVD coatings on titanium. Biomedical engineering online. 2006;5(1):1-10. 10.1186/1475-925X-5-22

24. Jokar K, Elmkhah H, Fattah-alhosseini A, Babaei K, Zolriasatein A. Comparison of the wear and corrosion behavior between CrN and AlCrN coatings deposited by Arc-PVD method. Materials Research Express. 2019;6(11):116426. 10.1088/2053-1591/ab4645

25. Olia H, Ebrahimi-Kahrizsangi R, Ashrafizadeh F, Ebrahimzadeh I. Corrosion study of TiN, TiAlN and CrN multilayer coatings deposit on martensitic stainless steel by arc cathodic physical vapour deposition. Materials Research Express. 2019;6(4):046425. 10.1088/2053-1591/aaff11

26. Khan MF, Adesina AY, Gasem ZM. Electrochemical and electrical resistance behavior of cathodic arc PVD TiN, CrN, AlCrN, and AlTiN coatings in simulated proton exchange membrane fuel cell environment. Materials and Corrosion. 2019;70(2):281-92. 10.1002/maco.201810377

27. D'Avico L, Beltrami R, Lecis N, Trasatti SP. Corrosion behavior and surface properties of PVD coatings for mold technology applications. Coatings. 2018;9(1):7. 10.3390/coatings9010007

28. Vengesa Y, Fattah-alhosseini A, Elmkhah H, Imantalab O, Keshavarz MK. Investigation of corrosion and tribological characteristics of annealed CrN/CrAlN coatings deposited by CAE-PVD. Ceramics International. 2023;49(2):3016-29.

29. Mani SP, Agilan P, Kalaiarasan M, Ravichandran K, Rajendran N, Meng Y. Effect of multilayer CrN/CrAlN coating on the corrosion and contact resistance behavior of 316L SS bipolar plate for high temperature proton exchange membrane fuel cell. Journal of Materials Science & Technology. 2022;97:134-46. 10.1016/j.jmst.2021.04.043

30. Wang L, Zhang S, Chen Z, Li J, Li M. Influence of deposition parameters on hard Cr–Al–N coatings deposited by multi-arc ion plating. Applied Surface Science. 2012;258(8):3629-36.

31. Fazel ZA, Elmkhah H, Fattah-Alhosseini A, Babaei K, Meghdari M. Comparing electrochemical behavior of applied CrN/TiN nanoscale multilayer and TiN single-layer coatings deposited by CAE-PVD method. Journal of Asian Ceramic Societies. 2020;8(2):510-8.

32. Adesina AY, Gasem ZM, Madhan Kumar A. Corrosion resistance behavior of single-layer cathodic arc PVD nitride-base coatings in 1M HCl and 3.5 pct NaCl solutions. Metallurgical and Materials Transactions B. 2017;48:1321-32. 10.1007/s11663-016-0891-7

33. Kong J-Z, Hou T-J, Wang Q-Z, Yin L, Zhou F, Zhou Z-F, et al. Influence of titanium or aluminum doping on the electrochemical properties of CrN coatings in artificial seawater. Surface and Coatings Technology. 2016;307:118-24. https://doi.org/10.1016/j.surfcoat.2016.08.036

34. Ardila L, Moreno C, Sanchez J. Electrolytic removal of chromium rich PVD coatings from hardmetals substrates. International Journal of Refractory Metals and Hard Materials. 2010;28(2):155-62. https://doi.org/10.1016/j.ijrmhm.2009.07.008

35. Liao L, Gao R, Yang Z, Wu S, Wan Q. A study on the wear and corrosion resistance of high-entropy alloy treated with laser shock peening and PVD coating. Surface and Coatings Technology. 2022;437:128281. 10.1016/j.surfcoat.2022.128281

36. Oliveira V, Aguiar C, Vazquez A, Robin A, Barboza MJR. Improving corrosion resistance of Ti–6Al–4V alloy through plasma-assisted PVD deposited nitride coatings. Corrosion Science. 2014;88:317-27. https://doi.org/10.1016/j.corsci.2014.07.047

37. Chenghao L, Li'nan J, Chuanjun Y, Naibao H. Crevice corrosion behavior of CP Ti, Ti-6Al-4V alloy and Ti-Ni shape memory alloy in artificial body fluids. Rare Metal Materials and Engineering. 2015;44(4):781-5. https://doi.org/10.1016/S1875-5372(15)30046-1

38. Beliardouh NE, Bouzid K, Nouveau C, Tlili B, Walock MJ. Tribological and electrochemical performances of Cr/CrN and Cr/CrN/CrAlN multilayer coatings deposited by RF magnetron sputtering. Tribology International. 2015;82:443-52. 10.1016/j.triboint.2014.03.018
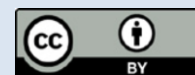
Persian Abstract

چکیده

در سال‌های اخیر از کاشتنی‌ها به عنوان پروتز برای جایگزینی و محافظت از استخوان استفاده می‌شود. تیتانیوم، به عنوان یک ماده کاشتنی، برای عملکرد بهتر نیاز به بهبود خواص خوردگی و سایش دارد. بنابراین، در مطالعه حاضر پوشش‌های نیترید با هدف بهبود خواص خوردگی و سایش بر زیرلایه تیتانیومی اعمال شدند. روش رسوب فیزیکی بخار تبخیر قوس کاتدی (CAE-PVD) برای رسوب پوشش های نانولایه CrN/CrAlN بر روی زیرلایه‌های تیتانیوم خالص تجاری و آلیاژ Ti6Al4V برای کاربردهای بیومواد استفاده شد. از پراش پرتو ایکس (XRD) برای مشخص کردن ساختار بلوری پوشش و از میکروسکوپ الکترونی روبشی (SEM) و میکروسکوپ الکترونی نشر میدانی (FESEM) برای مشاهده مورفولوژی سطح و سطح مقطع پوشش استفاده شد. چسبندگی پوشش طبق استاندارد VDI 3198 با استفاده از فرورونده Rockwell-C اندازه‌گیری شد. رفتار خوردگی توسط پلاریزاسیون پتانسیودینامیک و امپدانس الکتروشیمیایی طیف‌سنجی در محلول رینگر ارزیابی شد. نتایج نشان داد که پوشش نانولایه پتانسیل خوردگی را از V 0/368- به V 0/054- برای نمونه تیتانیوم و از V 0/405- به V 0/028- برای نمونه Ti6Al4V تغییر داد. علاوه‌براین، چگالی جریان خوردگی برای نمونه های پوشش داده شده تیتانیوم و Ti6Al4V به ترتیب به حدود یک هشتم و یک سوم کاهش یافت. قطر دایره خازن به دلیل رسوب پوشش CrN/CrAlN افزایش یافته است، که نشان دهنده رفتار خوردگی بهبود یافته نمونه‌های پوشش داده شده در مقایسه با نمونه های بدون پوشش است، زیرا پوشش به عنوان مانعی در برابر نفوذ محلول خورنده به زیرلایه عمل می کند.